

THESIS FOR THE DEGREE OF LICENTIATE OF ENGINEERING
IN
THERMO AND FLUID DYNAMICS

**Turbulent Shear Flow
Experiments: Design of
Natural Convection Rig and
LDA Measurement in
Swirling Jets**

ABOLFAZL SHIRI

Department of Applied Mechanics

CHALMERS UNIVERSITY OF TECHNOLOGY

Göteborg, Sweden, 2006

**Turbulent Shear Flow Experiments: Design of Natural Con-
vection Rig and LDA Measurement in Swirling Jets**
ABOLFAZL SHIRI

© ABOLFAZL SHIRI, 2006

THESIS FOR LICENTIATE OF ENGINEERING no 2006:13
ISSN 1652-8565

Division of Fluid Dynamics
Department of Applied Mechanics
Chalmers University of Technology
SE-412 96 Göteborg, Sweden
Phone +46-(0)31-7721400
Fax: +46-(0)31-180976

Printed at Chalmers Reproservice
Göteborg, Sweden 2006

Turbulent Shear Flow Experiments: Design of Natural Convection Rig and LDA Measurement in Swirling Jets

by

Abolfazl Shiri

abolfazl.shiri@chalmers.se

Division of Fluid Dynamics

Department of Applied Mechanics

Chalmers University of Technology

SE-412 96 Göteborg

Sweden

Abstract

This work consist of two sections. In the first part, a facility has been installed and modified from an existing rig in order to measure velocity and temperature field of axisymmetric turbulent natural convection boundary layers. With using laser doppler anemometry and cold wire resistance thermometry. A vertical aluminum pipe, heated by circulating water, creates a boundary layer around its outer surface which at the upper region of its $4.5m$ height becomes turbulent with a high Grashof number ($Gr_z > 10^{11}$). A vertical tunnel confines the flow from ambient, and air enters uniformly into the tunnel from below by using a set of vanes after it passes through three rows of screen and an axisymmetric contraction to decrease the turbulence intensity of air. The air is collected at the top section of rig and carried to the tranquillity chamber.

In the second part, incompressible swirling jets at different swirl numbers have been studied using the same experimental method as the first part. This experiment supplied the empirical data for a similarity study on the far-field of free jets with and without initial tangential velocity. The effects of different swirl numbers have been studied on the growth rate and velocity distribution of jet. The result shows the same self-similar solution for swirling and non-swirling axisymmetric jet. The tangential momentum displaces the virtual origin as soon as the swirl number exceeds $S > 0.2$.

Keywords: Natural Convection Boundary Layer, Laser Doppler Anemometry, Axisymmetric Jet, Swirl Number, Self-Similar Solution.

List of Publications

Based on the results of LDA experiments on shear flows, the appended papers were prepared:

- A.F. Shiri, W.K. George, J.W. Naughton, 2006, An Experimental Study of the Far-Field of Incompressible Swirling Jets, *The 36th AIAA Fluid Dynamics Conference and Exhibit*, June 5-8, San Francisco, California, USA.
- T.G. Johansson, F. Mehdi, A.F. Shiri, J.W. Naughton, 2005, Skin Friction Measurements Using Oil-Film Interferometry and Laser Doppler Anemometry, *4th AIAA Theoretical Fluid Mechanics Meeting*, June 6-9, Toronto, Ontario, Canada.

Preface

In first part of this Licentiate thesis, we have a report of the progress of the facility design and installation of *Turbulent Natural Convection Boundary Layer* Project. The initial installation and modifications of the experimental rig are finished and preliminary measurements are underway. The motivation for the project will be reviewed and the experimental facility described.

In second part we report on *Incompressible Swirling Jets* were initiated during the master project of A. Shiri, and have been extended as part of this work for two reasons: First high quality measurement on swirling flows are in and of themselves of great interest. Second these experiments have given us the necessary insight and experience with the LDA measurement technique.

This project has been funded by Swedish Research Council (*Vetenskapsrådet*) and has been carried out in the Department of Applied Mechanics, Chalmers University of Technology.

Acknowledgments

I would like to acknowledge my advisor Professor William K. George for his support and guidance throughout the course of this work. Working in his group is like spending time with relatives and family.

Also I would like to thank Professor Jonathan Naughton for his ideas and knowledge of experimental works. This thesis would never have reached to this point without his enlightening discussion and brilliant advices.

Special acknowledgment is made to Professor Gunnar Johansson for his on-time help, even on weekends.

Thanks for all the help and supports that I received from my great colleagues: Murat, Maja, Lars-Uno and Carlos, in the Turbulence Research Laboratory.

Lastly, but first in my thoughts, to my wife Maryam, for giving me her love and support during this time.

Nomenclature

Upper-case Roman

A, B_u, C	growth rate constants for self-preserving axisymmetric jet
D	nozzle exit diameter
G	degree of swirl $\equiv \frac{W_{max0}}{U_{max0}}$
G_θ	axial component of angular momentum flux
Gr_L	Grashof number based on the length
\mathcal{T}_{int}	integral time scale
L	axial length scale
\mathcal{L}	integral length scale
M_x	axial momentum flux
Nu	Nusselt number
N_{eff}	number of effectively independent samples
P	mean static pressure
P_a	ambient pressure
Pr	Prandtl number
Re_D	Reynolds number based on the jet diameter
R	nozzle exit radius
S	swirl number $\frac{G_\theta}{M_x R}$
T	temperature
T	total measurement time
U, V, W	mean axial, radial and tangential velocity components in the flow, respectively
U_0	average exit axial velocity

Lower-case Roman

f	frequency
f	normalized axial velocity function in the momentum integral
g	normalized azimuthal velocity function in the momentum integral
m_x	mass flux in axial direction
p	pressure
t	time

u	axial velocity component
v	radial velocity component
w	tangential velocity component
x, r, θ	cylindrical coordinate system
x_i	cartesian coordinate vector component
x_o	virtual origin for self-preserving axisymmetric jet

Lower-case Greek

α	thermal diffusivity
β	volumetric thermal expansion coefficient
$\delta_{1/2}$	jet half-width
$\epsilon_{\psi_N}^2$	relative statistical error of estimator ψ_N
ϵ_ν	viscous dissipation
η	normalized radial coordinate in the momentum integral
μ	viscosity
ν	kinematic viscosity ($\nu = \mu/\rho$)
ρ	density

Subscripts

c	center line
max	maximum value
o	jet, nozzle exit condition
∞	free stream or ambient conditions
$*$	scaled property

Superscripts

$'$	fluctuating quantity
-----	----------------------

Symbols

$\langle \dots \rangle$	time averaged quantity
-------------------------	------------------------

Abbreviations

CFD	Computational Fluid Dynamics
DNS	Direct Numerical Simulation
LDA	Laser Doppler Anemometry
RANS	Reynolds Averaged Navier-Stokes

Contents

Abstract	iii
List of Publications	v
Preface	vii
Acknowledgments	ix
Nomenclature	xi
I Natural Convection Experiment	1
1 Introduction on Natural Convection Rig	3
1.1 Motivation	3
1.2 Previous Research	4
1.3 Turbulent Natural Convection Boundary Layer	5
2 Design and Installation of Experiment	7
2.1 Modifications	9
2.2 Installation	11
3 Future Works	15
II Incompressible Swirling Jets	17
4 Introduction on Turbulent Swirling Jets	19
4.1 Incompressible Axisymmetric Jets	19
4.2 Self-similar (or Equilibrium Similarity) Analysis of Jet flow	20
4.3 Swirling Jet	22
4.4 The Goal of This Study	24
5 Momentum Equations in Cylindrical Coordinate	25

Part I

**Natural Convection
Experiment**

Chapter 1

Introduction on Natural Convection Rig

1.1 Motivation

Understanding the nature of buoyancy-driven flow next to a heated vertical surface has long been a challenging area of research in the field of Fluid Dynamics and Heat Transfer. Classical explanations and empirical relations with low level of accuracy can not answer the progressive needs of new technological applications. Efficient domestic heating and ventilation, compact heat sinks in electronic devices, passive control heat transfer in reactors and many other subjects would benefit from a complete understanding of natural convection heat transfer.

Despite numerous investigations and theoretical studies on the *Turbulent Natural Convection Boundary Layer*, there is a lack of reliable experimental data. As a result numerical analysis and modeling of the phenomena proceed without realistic guidelines. The usual assumptions and conditions are far from the actual behavior of this flow. Additional considerations on this matter, such as new properties, scaling factors and new theories of boundary layer, are needed.

The Department of Applied Mechanics, Chalmers University of Technology, has an on-going project that studies natural convection boundary layer with numerical methods such as DNS and LES (Barhaghi (2004)). The goal of this work is to provide a complementary experimental data with which numerical models can be validated through comparison.

In this study, we confine our attention to the turbulent natural convection boundary layer next to a heated wall. In order to simulate a two dimensional flow, instead of using semi-infinite vertical wall, we are using a cylindrical axisymmetric surface (a long pipe outer surface). The

are several reasons for this particular choice of experiment. First of all, it is a flow case which has been studied before with only limited degree of success (Tsuji & Nagano (1988a)). Second, we can measure with sufficient details the complicated near-wall flow to provide new physical insight as well as new experimental information. Third, it is a generic flow case, which means that the obtained results have general validity, Therefore it would be valuable as test case for CFD validation and further development of turbulence models.

The objective of this study is to carry out a turbulent natural convection experiment at high Grashof number ($\sim 10^{11}$), and perform detailed measurements of velocity and temperature in well-controlled environment. The experiment will use LDA and cold-wire resistance thermometry techniques.

1.2 Previous Research

Basic studies of turbulent natural convection along heated vertical flat plates were performed by Cheesewright (1968), Cheesewright & Ierokipitis (1982) and Tsuji & Nagano (1988a). Cheesewright (1968) used hot-wire anemometry and cold wire resistance thermometer to measure mean and fluctuating velocity and temperature, and his study was the most comprehensive at the time. Later on, however, it was shown by Hoogendoorn & Euser (1978) that the energy balance for the boundary layer was not satisfied, and that the most likely error was in the velocity measurements. This was later confirmed and is also easy to understand: using hot-wires in flows with large velocity and temperature fluctuations requires a very good separation of these fluctuations, which is extremely difficult to do.

The accuracy problem with hot-wires in thermal flows is caused by the physics of the method and therefore can not easily avoided. The velocity magnitudes of buoyancy-driven flows are in the range of $1m/s$. Therefore the natural convective heat transfer of the wire itself has an effect on the velocity field. Turbulence data obtained with hot-wires in buoyant flows therefore suffer from large uncertainties, particularly in boundary layers (close to the wall). This also has been seen, for example, in the experimental data of Tsuji & Nagano (1988a). In spite of this, their experiment is used as test case for validating turbulence models, since there were no other alternatives. The remedy to the problem of uncertainty in the velocity measurement is to replace the hot-wire techniques of previous experiments with laser Doppler anemometry (*LDA*) which can produce highly accurate results.

There are other problems with the earlier experiments as well. Many

of the previous studies of the natural convection boundary layer have been made in flows along vertical plates which attempted to simulate infinite surface (Cheesewright (1968); Cheesewright & Ierokipitis (1982); Kato *et al.* (1993); Tsuji & Nagano (1988*b*)) or in flows confined in slender cavities (Elder (1965)). In vertical flat plate experiments, it is hard to eliminate the effect of side walls. Also stratification of the flow is caused by the finite surroundings. The problem encountered in the slender cavity between parallel surfaces is that these flows tend to create recirculation cells and be very dependent on flow geometry (especially aspect ratio) which leads us to a different and very complicated flow regime that is not in our interest. These difficulties led us to the alternative geometry used in this study, which is the axisymmetric wall.

1.3 Turbulent Natural Convection Boundary Layer

Turbulence is characteristic state of a flow in which scalar transport such as heat and mass transfer are enhanced compared to laminar flow sometimes by many orders of magnitude. Natural convection flows are caused by the density variations, most frequently related to temperature differences, together with the acceleration of gravity. In the presence of a boundary (like a vertical heated wall) the flow creates a boundary layer along the wall which starts from bottom to the top of the vertical wall. As far as the flow moves up along the wall, the boundary layer will evolve from a steady, laminar flow into a transition region, and if the wall is high enough it will become a fully turbulent boundary layer.

The dimensionless parameter which defines the evolution of the buoyancy-driven flow in the vicinity of a vertical heated wall is the Grashof number given by:

$$Gr_x \equiv \frac{g\beta(T_w - T)x^3}{\nu^2} \quad (1.1)$$

where g is the acceleration of gravity, ν is the kinematic viscosity, $(T_w - T)$ is the difference between the local temperature and wall temperature, β is the thermal expansion coefficient and x is the vertical distance along the wall. The Grashof number can be interpreted as a ratio between "buoyant forces" and "viscous forces", and is based on a vertical length scale, x . The experimental results show that the criterion for the beginning of turbulence in natural convection is a range of Grashof

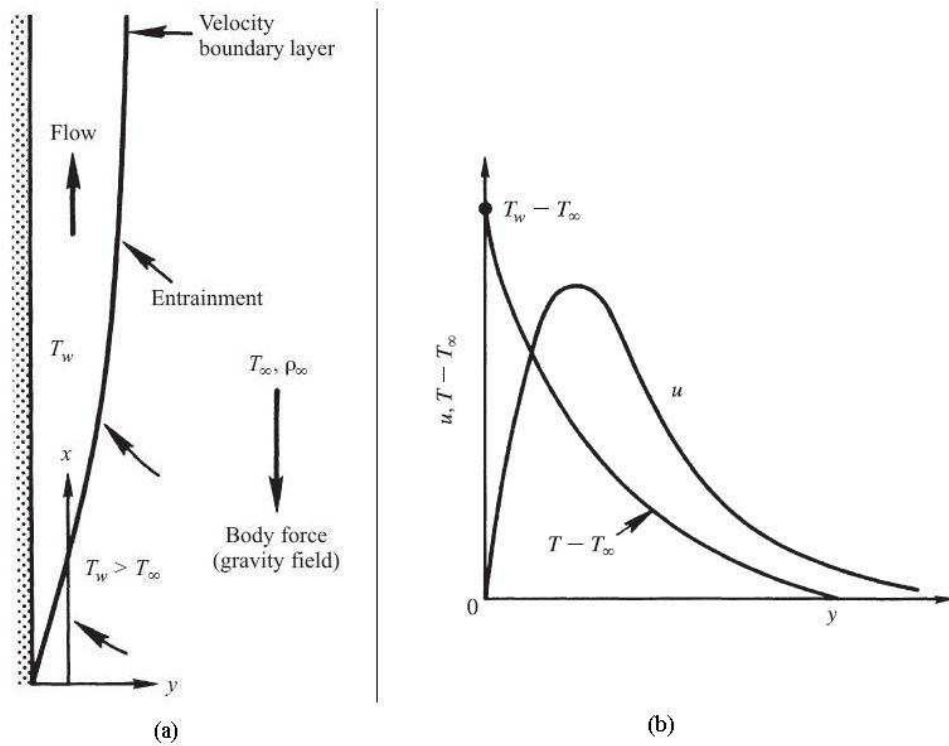


Figure 1.1: (a)Boundary layer created on a vertical hot wall; (b)Velocity and temperature distribution profile in the boundary layer.

numbers between 3.5×10^8 to 1.5×10^{10} (see Gebhart & Jaluria (2003)).

Chapter 2

Design and Installation of Experiment

The experimental facility is a modification of the tunnel which was used in the Persson & Karlsson (1996) experiment, and was a partially enclosed 2.5m high heated vertical cylinder. The cylinder was enclosed by four vertical walls with a small gap between the floor and the lower edge of the walls, so that the air could enter the enclosure through the gap. There was no roof on the enclosure, so that the heated air could rise far above the height of the cylinder in order to maintain zero vertical temperature stratification. In the previous setup the Grashof number that could be achieved was too low to permit fully turbulent flow over a sufficient portion of the cylinder. The velocity data, while it was measured simultaneously with temperature, had some deviation from data without temperature measurement, probably caused by cold-wire probe blockage.

As it is shown in figure 2.1, a new design has been made for the rig in order to achieve the goals of this project and eliminate the deficiencies in the measurement. This is a test rig for natural convection, but with a small component of mixed convection as well. The reason for additional pressure gradient on the system is that to avoid the air recirculation inside the tunnel and make the desired test case similar to the heated vertical cylinder in infinite, unstratified and undisturbed surroundings. Also in any building there is a small draft from the openings or air-conditioning which can have an impact on the low velocity flow field of a natural convection experiment. To separate the air flow from temperature stratification in the room, a fiberglass tunnel concentric with cylinder has been used. By controlling the air flow, the co-flow can be adjusted to zero at a given height, thereby permitting a certain amount of control of the stratification.

The tunnel is enclosed by an inlet chamber from bottom and a col-

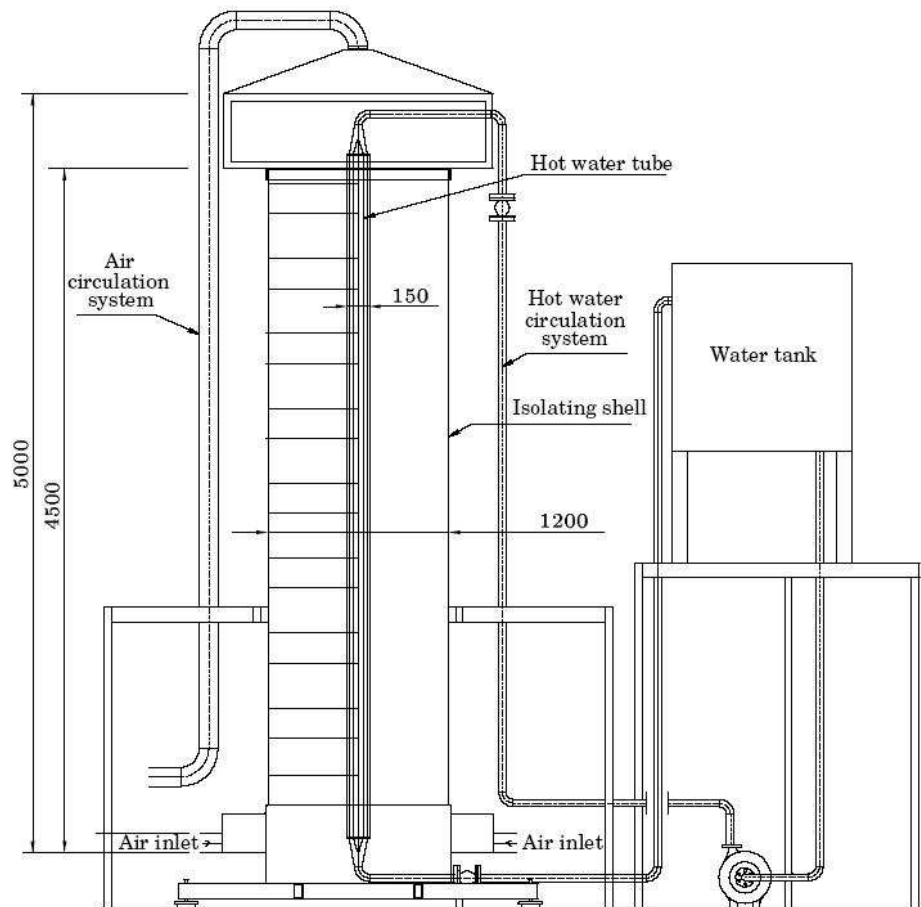


Figure 2.1: Installation Layout.

lection hood on top of the rig. The vertical aluminium cylinder (150mm outer diameter and 4500mm height) is heated by water circulating inside the cylinder through hot-water circulation system including a pump and a water reservoir with electrical heating capability. The water flow is large enough so that the cylinder can be considered isothermal. The maximum cylinder temperature is about 80 degree centigrade, giving a maximum Grashof number of about 4×10^{11} at the height 4m.

The air flow circulates from the inlet chamber at the bottom and the collection hood at the top of the rig then passes through a HVAC unit to be cooled down and is passed back to the air inlet by using a small fan.

Air is used as fluid in order to avoid the large refraction-index variations that occur in water flows with density variations and makes it practically impossible to use optical methods for velocity measure-

ments. For the detailed mean flow and turbulence measurement, a LDA method is used. The spatial resolution of the LDA is less than 0.2mm normal to the wall. Mean and fluctuating temperature will be measured with small (1mm long and 1micron diameter) cold-wires resistance thermometers. The laser probe moves with the temperature sensor on the same traverse system to provide simultaneous data from the velocity field and temperature field. With this technique we can measure the mixed velocity-temperature moments at almost zero separation and very close to the wall (less than one viscous length).

2.1 Modifications

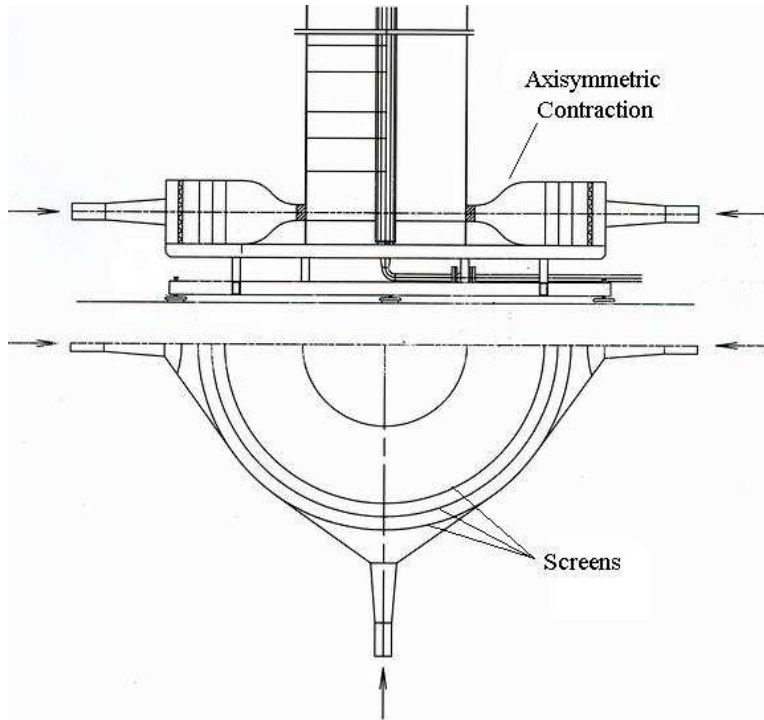


Figure 2.2: Modifications on inlet chamber; Layout.

Unfortunately for the flow case with theoretically infinite surroundings, zero temperature stratification is very difficult (if not impossible) to simulate experimentally, because of the finite entrainment rate at large distance from the surface. In fact, what one really has studied is the flow in a large cavity, with the usual result that a thermal stratification (vertical temperature gradient) is set up in the cavity. the entrainment of this stably stratified external flow seriously erodes the

Abolfazl Shiri, Turbulent Shear Flow Experiments: Design of Natural Convection Rig and LDA Measurement in Swirling Jets

buoyancy integral which drives the flow, and considerably complicates the energy balance. This led us to make a number of modifications on the experimental facility to remove the deficiencies.

Initial measurements on the inlet flows showed a velocity variation about 10% around the perimeter. Such a large variation was considered unacceptable because the axisymmetric condition was not satisfied. In order to control the inlet condition, an axisymmetric contraction together with three rows of concentric perforated plates has been designed and manufactured by Karlson and Axelsson (2003). (see figures 2.2 and 2.3). The new inlet chamber section has the ability to control the flow rate and give a uniform entrance profile for inlet flow. The air is uniformly distributed around the perimeter so that the inlet flow becomes horizontal and directed radially inward. Now we can produce an axisymmetric flow around the cylinder, with well-defined inlet and outlet boundary conditions.



Figure 2.3: Axisymmetric inlet to the tunnel.

The collection hood has been designed to separate the tunnel from its surroundings, and also with its symmetric shape, decrease the effect of non-uniform outflows. A perforated plate inside the collection hood also helps to eliminate the large scale instabilities. Figure 2.4 shows the section of collection hood in its final position.



Figure 2.4: Natural convection rig; collection hood.

2.2 Installation

The *natural convection rig* was installed in the Fluid Dynamics Laboratory of the Department of Applied Mechanics. As it can be seen in figures 2.4-2.6, it is positioned in the basement through an opening in the ceiling gives the necessary height for the $7m$ high rig.



Figure 2.5: Natural convection rig; tunnel and inlet chamber.

CHAPTER 2. DESIGN AND INSTALLATION OF EXPERIMENT



Figure 2.6: Natural convection rig; hot water piping and air circulation housings.

Abolfazl Shiri, Turbulent Shear Flow Experiments: Design of Natural Convection Rig and LDA Measurement in Swirling Jets

Chapter 3

Future Works

The facility described in last chapter is now installed, based on the modifications, in the department of Applied Mechanics laboratory, Chalmers university of Technology, and is being tested for its defined conditions. The tests which have to be performed in order to create a approved case of study are listed below:

- **Uniform in-flow:**
The inlet should distribute a symmetric uniform air flow on the heated surface. A series of experiments are needed to insure the efficiency of the new design. Both qualitative (flow visualization) and quantitative (hot-wire anemometry) methods have been designed to be performed.
- **Effect of new modification on the stratified flow inside the tunnel:**
The stratification can be controlled partially by controlling the inlet air flow rate. the temperature in different regions of the tunnel should be measured at the same time to have a optimum desirable situation.
- **Undesirable pressure and temperature gradient caused by ambient:**
The ambient temperature varies in different heights of the rig. The isolation of the tunnel should be tested both for leakage and conduction heat transfer. Also the cylinder should be monitored to obtain a steady isothermal surface during measurement.
- **Reliability of the techniques to perform LDA and cold-wire measurement:**
Another challenge for cold-wire measurement at the same time with the LDA with the necessary spacial resolution is that the laser beams focuses a considerable amount of energy in a small

Abolfazl Shiri, Turbulent Shear Flow Experiments: Design of Natural Convection Rig and LDA Measurement in Swirling Jets

region and warms up the air inside the measurement volume. Adjusting the cold-wire to a position to reduce the effect of laser heat is a crucial issue to be considered.

Part II

Incompressible Swirling Jets

Chapter 4

Introduction on Turbulent Swirling Jets

This chapter and the next one provide an introduction to turbulent swirling jets. The discussion of the new theory, the experiment performed, and the results are reported in the appended paper prepared for the AIAA Fluid Dynamics meeting in San Francisco, June 5-8, 2006.

4.1 Incompressible Axisymmetric Jets

Incompressible jet flows are one of the most common types of the free turbulence which can be defined as a high-Reynolds-Number shear flow in an open ambient fluid, unconfined or uninfluenced by walls. When fully-developed, the mean velocity profile can be described by a characteristic velocity scale, $U_{max}(x)$, and a characteristic shear layer width, $\delta_{1/2}(x)$. The growth rate, $d\delta/dx$ and profiles of the turbulence intensities have been shown to depend on the manner in which they are generated, even in an infinite environment.

Since these flows are "free", or unconfined, the pressure is approximately constant throughout the flow, except for small turbulent fluctuations within the shear layer. We are looking in our experiments for the asymptotic downstream behavior of the free turbulent jet. Until relatively recently, it was traditionally assumed that such jets were independent of the exact type of source which created the flow. However, George (1989) demonstrated that the equations that govern the evolution of the mean velocity and the turbulent kinetic energy admit similarity solutions that are dependent on the initial conditions of the jet. The experimental measurements of Hussein *et al.* (1994) and Panchapakesan & Lumley

(1993) are in excellent agreement with the similarity hypothesis. Figure 1-1 shows the details of the initial formation of a jet, assuming a still ambient fluid. The figure is valid only for similar jet and ambient fluids, e.g., air-into-air. Typically the jet issues with a nearly flat, fully developed turbulent velocity profile at velocity U_0 , a so-called 'top-hat' jet. Mixing layers form at the lip of the exit, growing between the still ambient and the nearly inviscid potential core, also flowing at velocity U_0 . In low Mach number jets, the potential core vanishes quickly at a distance of about three diameters from the exit, and the velocity profile loses its mixing-layer flat-core shape. The length of the potential core increases as the Mach number increases, and a similar thing happens for very low Reynolds number jets as well (less than a few thousand).

Downstream of the potential core, the flow begins to develop into the distinctive Gaussian-type profile we think of as a "jet". Finally, at about 20 diameters downstream of the exit, the mean velocity profile reaches and maintains a self-preserving shape. It is this asymptotic self-similar form of free turbulent flows which we wish to study.

Properly normalized profiles of statistical quantities will collapse together reasonably well. The developed or self-similar region seems to grow from an apparent origin near the exit. Also the velocity profiles in different cross-section of jet have the same momentum but not the same mass flow. Fluid is entrained into the jet from the ambient region and the jet mass flow increases downstream.

Turbulence is three-dimensional by nature; therefore any geometrical simplification in the flow, like symmetries, will help reduce the complexity of the problem, especially when working with average quantities. The simplest jet flow, which can be measured in a real experiment, would be a two-dimensional jet flow. Eliminating the third dimension by symmetry, imposes an axisymmetric flow which can be studied in cylindrical coordinate.

4.2 Self-similar (or Equilibrium Similarity) Analysis of Jet flow

Assume that we are sufficiently far downstream for the jet velocity profiles to become self-similar so that all profiles can be written as:

$$T(x, r) = T_x(x)F(r/\delta) \quad (4.1)$$

where T can be any statistical quantity, F is a normalized profile which depends only on the dimensionless coordinate, r/δ , and δ is the

CHAPTER 4. INTRODUCTION ON TURBULENT SWIRLING JETS

appropriate length scale which increases with x . Every statistical quantity has its own scale function, but all share the same length scale. For example, the mean velocity and Reynolds stress profiles can be written as:

$$U(x, r) = U_s(x)f(r/\delta) \quad (4.2)$$

$$-\langle uv \rangle = R_s(x)g(r/\delta) \quad (4.3)$$

It is convenient to choose $U_s = U_c$, the velocity at the centerline, and $\delta = \delta_{1/2}$, the radius at which the mean velocity equals half its centerline value. The scale for the Reynolds stress, R_s , like most other statistical quantities is more problematical, and must be deduced by applying equilibrium similarity assumptions to the data. In fact, $R_s = U_s^2 d\delta/dx$, but since the jet can be shown to grow linearly, it can be taken as just U_s^2 with the small price that the coefficient can depend on the source conditions.

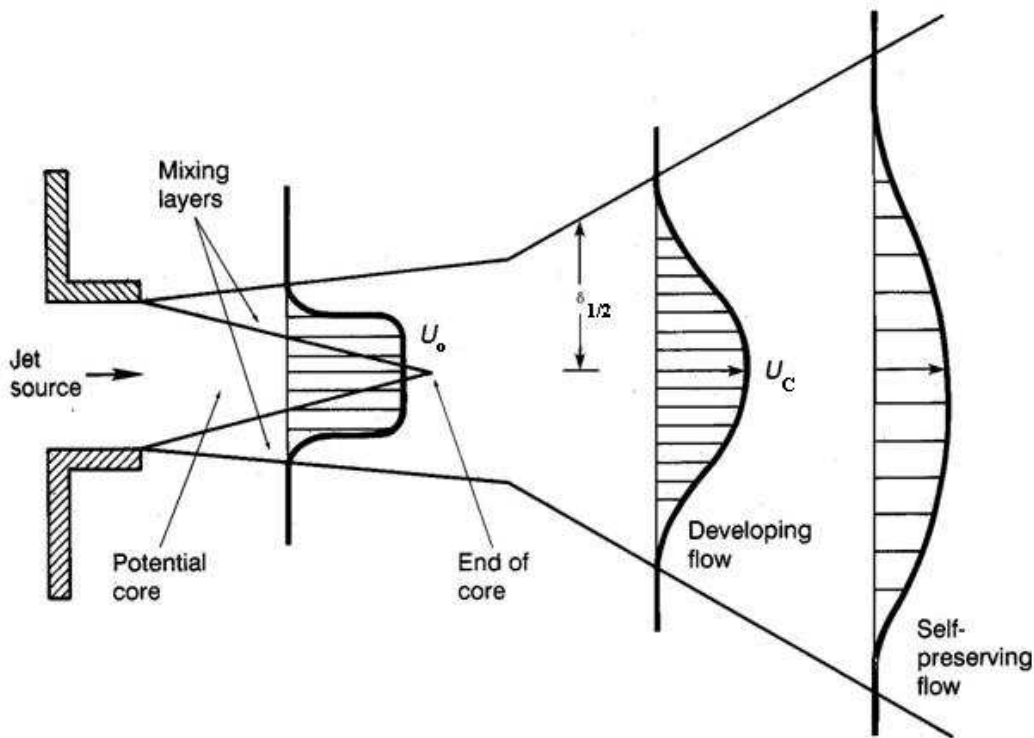


Figure 4.1: Details of the early development of a real jet.

In the self-similar region it can be shown by considering the second moment RANS equations that:

$$\delta_{1/2} = A(x - x_o) \quad (4.4)$$

where A is a constant at most dependent on the source conditions, and x_o is the afore-mentioned virtual origin. The constant, $A = d\delta_{1/2}/dx$, is not unique, which means that the growth rate for all self-similar turbulent jets can depend on the source condition.

In spite of the dependence of the spreading rate on the upstream conditions, the velocity profile, however, can be shown to be universal and independent of source conditions when normalized by the centreline velocity and half-width. This is illustrated with experimental data in figure 4.2.

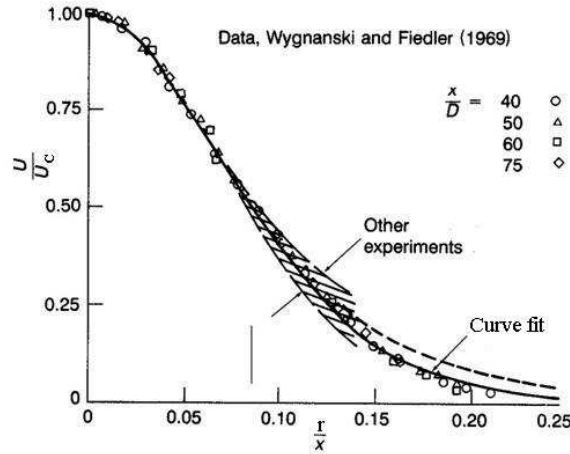


Figure 4.2: early results of normalized velocity profiles compare to *sech* curve fit.

Self-similarity in the velocity profile occurs downstream after the statistics of the flow have gone through their internal adjustments and the various terms in the RANS equations have reached equilibrium with respect to each other. For most jets, this usually happens after $x/D > 20$ for mean velocities; however the turbulence components can sometimes take longer to become self-similar.

4.3 Swirling Jet

In many fluid dynamic applications (including combustion and active control of separation), swirling jet flows are used due to their unique flow field properties. In combustors swirl is often added to modify the

CHAPTER 4. INTRODUCTION ON TURBULENT SWIRLING JETS

entrainment and mixing processes. Also swirling jet flows can be created as by-products of flows through turbomachinery.

Although the swirling jet flows are common, there are still some aspects of it that are not well understood and need reliable theories to explain. For example, swirling jet flows exhibit increased growth rates compared to pure axial-flow jets, but the mechanism behind the increased growth rate has yet to be explained.

Although the development of the near field is often of more interest in engineering applications, features of far field, such as growth rate, are used to test turbulence models. It is also straightforward to compare the modeled and measured velocity and Reynolds stress profiles in this region if we have self-similarity in the far field.

Imposing an additional component of strain on a turbulent flow, like curvature on a turbulent boundary layer, can create larger effects on the flow than would be predicted by the simple increase in total strain (Gilchrist and Naughton 2005). It can have an order-of-magnitude greater effect on skin friction than does the same curvature acting on laminar boundary layer. It has been suggested that the additional terms that appear in the equations of motion, particularly the Reynolds stresses equation, cause changes in the turbulence structure. In the jet flow, adding a component of strain in a direction perpendicular to the strain produced by the jet's axial velocity could cause a large change in the jet growth rate. This additional strain in a round jet is created by tangential momentum, thereby producing a swirling jet flow, which imposes pressure gradients on the flow that are required to support the flow curvature in the jet.

In most cases, the experimental results have shown that swirling jets exhibit more rapid growth than their non-swirl counterparts. This enhanced growth has been attributed to the centrifugal instability present in the flow that increases the stream-wise vorticity present in the mixing layer. The effect of swirl also increases with compressibility, which is because of the increased importance of the stream-wise vortices as the effect of tangential vorticity decreases.

One of the variables affecting growth rate in swirling flows that is not well understood is the initial swirl profile at the exit. Only a few experimental studies have investigated an unconfined jet with multiple swirl profiles, and those have only been done at one swirl strength. Recently, direct numerical simulation (Hu and Sun 2001) has been used to compare different tangential velocity profiles. However, the generation of several different swirl profiles in an experimental facility is not easily accomplished. For instance, rotating pipes produce only one type of swirl profile, and vane systems require

a change of vane geometry to produce different flows.

4.4 The Goal of This Study

The main goal of this work is to investigate the effect of swirl strength on jet growth rates using LDA flow field measurements in the far field and also the developing region of a jet flow. Although there are many studies of swirling jet flows, there are few studies that have investigated incompressible swirling free jets over the range of conditions and in the detail provided by the present study.

To generate the different swirl profiles investigated in this study, a facility has been constructed that allows for control of the tangential velocity profile and the creation of a swirling jet that is largely free from artifacts produced by the swirl generation process. This was accomplished by using two blowers to produce main jet flow and the rotational flow separately.

Chapter 5

Momentum Equations in Cylindrical Coordinate

To study a symmetrical flow field, we start with Navier-Stokes equations in cylindrical coordinate. Also the assumption of a steady, incompressible, and Newtonian flow matches with our case studies.

$$\frac{1}{r} \frac{\partial}{\partial r}(rV_r) + \frac{1}{r} \frac{\partial V_\theta}{\partial \theta} + \frac{\partial V_z}{\partial z} = 0 \quad (5.1)$$

$$V_r \frac{\partial V_z}{\partial r} + \frac{V_\theta}{r} \frac{\partial V_z}{\partial \theta} + V_z \frac{\partial V_z}{\partial z} = \quad (5.2)$$

$$\begin{aligned} & -\frac{1}{\rho} \frac{\partial \tilde{P}}{\partial z} + \nu \nabla^2 V_z \\ V_r \frac{\partial V_r}{\partial r} + \frac{V_\theta}{r} \frac{\partial V_r}{\partial \theta} + V_z \frac{\partial V_r}{\partial z} - \frac{V_\theta^2}{r} = & \quad (5.3) \end{aligned}$$

$$\begin{aligned} & -\frac{1}{\rho} \frac{\partial \tilde{P}}{\partial r} + \nu \left(\nabla^2 V_r - \frac{V_r}{r^2} - \frac{2}{r^2} \frac{\partial V_\theta}{\partial \theta} \right) \\ V_r \frac{\partial V_\theta}{\partial r} + \frac{V_\theta}{r} \frac{\partial V_\theta}{\partial \theta} + V_z \frac{\partial V_\theta}{\partial z} + \frac{V_r V_\theta}{r} = & \quad (5.4) \\ & -\frac{1}{\rho r} \frac{\partial \tilde{P}}{\partial \theta} + \nu \left(\nabla^2 V_\theta - \frac{V_\theta}{r^2} + \frac{2}{r^2} \frac{\partial V_r}{\partial \theta} \right) \end{aligned}$$

where:

$$\nabla^2 \equiv \frac{\partial^2}{\partial r^2} + \frac{1}{r} \frac{\partial}{\partial r} + \frac{1}{r^2} \frac{\partial^2}{\partial \theta^2} + \frac{\partial^2}{\partial z^2}$$

By using the Reynolds decomposition,

$$\begin{cases} \text{Axial Component (x):} & V_z = U + u \\ \text{Radial Component (r):} & V_r = V + v \\ \text{Azimuthal Component (\theta):} & V_\theta = W + w \\ \text{Azimuthal Component (\tilde{P}):} & \tilde{P} = P + p \end{cases}$$

using continuity equation, and averaging the equation above to involve Reynolds Stresses, we obtain the "Averaged Momentum Equations" in cylindrical coordinates as:

$$\begin{aligned} U \frac{\partial U}{\partial x} + V \frac{\partial U}{\partial r} + \frac{W}{r} \frac{\partial U}{\partial \theta} &= -\frac{1}{\rho} \frac{\partial P}{\partial x} + \nu \nabla^2 U \\ &\quad - \left\langle \frac{\partial u^2}{\partial x} + \frac{\partial uv}{\partial r} + \frac{1}{r} \frac{\partial uw}{\partial \theta} + \frac{uw}{r} \right\rangle \\ U \frac{\partial V}{\partial x} + V \frac{\partial V}{\partial r} + \frac{W}{r} \frac{\partial V}{\partial \theta} - \frac{W^2}{r} &= -\frac{1}{\rho} \frac{\partial P}{\partial r} + \nu \left(\nabla^2 V - \frac{V}{r^2} - \frac{2}{r^2} \frac{\partial W}{\partial \theta} \right) \\ &\quad - \left\langle \frac{\partial uv}{\partial x} + \frac{\partial v^2}{\partial r} + \frac{1}{r} \frac{\partial vw}{\partial \theta} - \frac{w^2}{r} + \frac{v^2}{r} \right\rangle \\ U \frac{\partial W}{\partial x} + V \frac{\partial W}{\partial r} + \frac{W}{r} \frac{\partial W}{\partial \theta} + \frac{VW}{r} &= -\frac{1}{\rho r} \frac{\partial P}{\partial \theta} + \nu \left(\nabla^2 W - \frac{W}{r^2} + \frac{2}{r^2} \frac{\partial V}{\partial \theta} \right) \\ &\quad - \left\langle \frac{\partial uw}{\partial x} + \frac{\partial vw}{\partial r} + \frac{1}{r} \frac{\partial w^2}{\partial \theta} + 2 \frac{vw}{r} \right\rangle \end{aligned}$$

For a statistically homogeneous flow in the azimuthal direction, $\partial/\partial\theta = 0$, the averaged continuity and momentum equations in an incompressible, the high Reynolds number, turbulent, round jet with swirl can be reduced to the equations below:

$$\begin{aligned} U \frac{\partial U}{\partial x} + V \frac{\partial U}{\partial r} &= -\frac{1}{\rho} \frac{\partial P}{\partial x} + \nu \nabla^2 U \\ &\quad - \left\langle \frac{\partial u^2}{\partial x} + \frac{\partial uv}{\partial r} + \frac{uw}{r} \right\rangle \end{aligned} \quad (5.5)$$

$$\begin{aligned} U \frac{\partial V}{\partial x} + V \frac{\partial V}{\partial r} - \frac{W^2}{r} &= -\frac{1}{\rho} \frac{\partial P}{\partial r} + \nu \left(\nabla^2 V - \frac{V}{r^2} \right) \\ &\quad - \left\langle \frac{\partial uv}{\partial x} + \frac{\partial v^2}{\partial r} - \frac{w^2}{r} + \frac{v^2}{r} \right\rangle \end{aligned} \quad (5.6)$$

$$\begin{aligned} U \frac{\partial W}{\partial x} + V \frac{\partial W}{\partial r} + \frac{VW}{r} &= \nu \left(\nabla^2 W - \frac{W}{r^2} \right) \\ &\quad - \left\langle \frac{\partial uw}{\partial x} + \frac{\partial vw}{\partial r} + 2 \frac{vw}{r} \right\rangle \end{aligned} \quad (5.7)$$

*CHAPTER 5. MOMENTUM EQUATIONS IN CYLINDRICAL
COORDINATE*

These equations have been analyzed in detail in Shiri (2004), using an order of magnitude analysis, so that analysis will not be repeated here. In brief, derivatives of averaged quantities in the x -direction are ignored relative to those in the cross-stream direction, and all viscous terms are neglected since the Reynolds number is presumed large. The final result when integrated over the entire cross-section leads to the momentum and angular momentum integrals given by:

$$M_x = 2\pi \int_0^\infty \left[U - \frac{W^2}{2} + \langle u^2 \rangle - \frac{\langle v^2 \rangle + \langle w^2 \rangle}{2} \right] r dr \quad (5.8)$$

$$G_\theta = 2\pi \int_0^\infty [UW + \langle uw \rangle] r^2 dr \quad (5.9)$$

These together form the basis of the AIAA paper which appended.

Bibliography

- AXELSSON, L. 2003 An investigation of buoyancy-driven turbulent flows. Master's thesis, Chalmers University of Tech.
- BARHAGHI, D. G. 2004 DNS and LES of turbulent natural convection boundary layer., licentiate thesis.
- CHEESEWRIGHT, R. 1968 Turbulent natural convection from a vertical plane surface. *Journal of Heat Transfer* **90**, 1–8.
- CHEESEWRIGHT, R. & IEROKIOPITIS, E. 1982 Velocity measurements in a turbulent natural convection boundary layer. In *Proceedings of the Seventh International Heat Transfer Conference*, , vol. II, pp. NC 31,305–309. Munich.
- ELDER, J. W. 1965 Laminar free convection in a vertical slot. *Journal of Fluid Mechanics* **23**, 76–98.
- GEBHART, B. & JALURIA, Y. 2003 *Buoancy-Induced Floes and Transport*. Stanford, California: Taylor and Francis.
- GEORGE, W. 1989 The self-preservation of turbulent flows and its relation to initial conditions and coherent structures. In *Advances in Turbulence* (ed. W. George & R. Arndt), pp. 39–73. New York: Springer.
- HOOGENDOORN, C. J. & EUSER, H. 1978 Velocity profiles in the turbulent free convection boundary layer. In *Proceedings of the Sixth International Heat Transfer Conference*, , vol. 2, pp. NC 2,193–198. Toronto.
- HUSSEIN, H. J., CAPP, S. P., & GEORGE, W. K. 1994 Velocity measurements in a high-reynolds-number, momentum-conserving, axisymmetric, turbulent jet. *Journal of Fluid Mechanics* **258**, 31–75.
- KATO, S., MURAKAMI, S. & YOSHIE, R. 1993 Experimental and numerical study on natural convection with strong density variation

Abolfazl Shiri, Turbulent Shear Flow Experiments: Design of Natural Convection Rig and LDA Measurement in Swirling Jets

along a heated vertical plate. In *9th Symposium on Turbulent Shear Flows, Kyoto, Japan*.

PANCHAPAKESAN, N. & LUMLEY, J. 1993 Turbulence measurements in axisymmetric jets of air and helium. part 1. air jet. *Journal of Fluid Mechanics* **246**, 197–223.

PERSSON, N. & KARLSSON, R. 1996 Turbulent natural convection around heated vertical slender cylinder. In *8th Int. Symposium on Application of Laser Techniques to Fluid Mechanics*. Lahaina, Hawaii.

SHIRI, A. 2004 An experimental study of incompressible swirling jets. Master's thesis, Chalmers University of Technology.

TSUJI, T. & NAGANO, Y. 1988a Characteristics of a turbulent natural convection boundary layer along a vertical flat plate. *Int. Journal of Heat Mass Transfer* **31** (8), 1723 – 1734.

TSUJI, T. & NAGANO, Y. 1988b Turbulence measurements in a natural convection boundary layer along a vertical flat plate. *Int. Journal of Heat Mass Transfer* **31** (10), 2101 – 2111.

Paper I

Paper II